frontiers | Frontiers in Nutrition

TYPE Original Research
PUBLISHED 11 July 2025
DOI 10.3389/fnut.2025.1616272

OPEN ACCESS

EDITED BY
Lijun Sun,
Northwest A&F University, China

REVIEWED BY
Ahmed A. Zaky,
National Research Centre, Egypt
Yu Xiao,
Hunan Agricultural University, China

*CORRESPONDENCE
Li Wen
✉ wl@csust.edu.cn

RECEIVED 22 April 2025
ACCEPTED 02 July 2025
PUBLISHED 11 July 2025

CITATION
Zhang Z, Bi X, Hu L, Wu Y, Hu W, Wang H, Zheng X, Wu H, Mu D, Wen L and Huang Q (2025) Enhancing antioxidant activity of rice protein hydrolysates through glycosylation modification.
Front. Nutr. 12:1616272.
doi: 10.3389/fnut.2025.1616272

Enhancing antioxidant activity of rice protein hydrolysates through glycosylation modification

Zhimin Zhang[1], Xinjian Bi[1], Liangjie Hu[1], Ying Wu[1], Wenting Hu[1], Han Wang[1], Xinyue Zheng[1], Hao Wu[1], Daichen Mu[1], Li Wen[1]* and Qingming Huang[2]

[1]School of Food Science and Bioengineering, Hunan Provincial Key Laboratory of Cytochemistry, Changsha University of Science and Technology, Changsha, China, [2]Hunan Zhunong Rice Industry Ltd Co., Yiyang, China

Objective: This work sought to improve the potential use of rice protein by examining the antioxidant activity of glycosylated rice protein hydrolysates (RPH).

Methods: RPH were produced via the enzymatic breakdown of rice protein powder utilizing trypsin. Then, using the Maillard reaction, these hydrolysates were glycosylated with three functional monosaccharides to create RPH-fructose (RPH-F), RPH-xylose (RPH-X), and RPH-arabinose (RPH-A). The antioxidant capabilities of glycosylated derivatives were assessed *in vitro* by measuring Fe^{2+} chelating ability and their ability to neutralize several radicals, including hydroxyl (•OH), superoxide anion (O_2•$^-$), 2,2-diphenyl-1-picrylhydrazyl radical (DPPH•), and 2,2′-azinobis (3-ethylbenzothiazoline-6-sulfonate) radical (ABTS•$^+$). A zebrafish *in vivo* model was utilized to investigate oxidative damage, analyzing the distribution of reactive oxygen species (ROS) through fluorescence staining and evaluating oxidative stress by quantifying malondialdehyde (MDA) levels and the activity of antioxidant enzymes such as catalase (CAT) and total superoxide dismutase (T-SOD). Following glycosylation, DPPH• clearance by RPH-X increased by 12.75% (6 mg/mL), and ROS inhibition by RPH-A in the zebrafish model reached 84.78%.

Conclusion: Glycosylation enhanced the antioxidant capabilities of rice protein hydrolysate, indicating its potential as a functional dietary component with antioxidant efficacy.

KEYWORDS

rice protease hydrolysate, Maillard reaction, zebrafish, antioxidant activity, glycosylation

1 Introduction

Oxidative stress primarily arises from an imbalance between oxidative and antioxidant mechanisms in the body. This imbalance leads to oxidation and the excessive production of ROS, including superoxide anions and hydroxyl radicals (1). These ROS damage cellular macromolecules, accelerating the aging process and leading to functional decreases in cells and tissues, as well as impairing physiological health (2). Therefore, the elimination of excess reactive oxygen species and the suppression of oxidative reactions are crucial goals in the creation of antioxidant products.

Altering glycosylation in diverse ways may modify bioactive peptides' structure and physicochemical properties, enhancing their biological activity. Three principal ways are utilized for glycosylation: enzymatic approach, non-covalent linkage, and Maillard reaction-based method. Transglutaminase (TGase) is the most often utilized enzyme in glycosylation processes. Song et al. used the TGase method to glycosylate soybean isolate protein (SPI) digest and found that the method significantly improved the *in vitro* antioxidant capacity of SPI (3). Nonetheless, its intricate manufacture and preparation method and low biocatalyst stability restrict its applicability (4). Non-covalent linkage methods entail the covalent bonding to particular amino groups of proteins or peptides, while weaker physical interactions facilitate the attachment of peptides to polysaccharides (5). Nevertheless, the majority of these compounds or derivatives frequently demonstrate instability. Zeng et al. compared various common glycosylation methods and reviewed the progress of glycosylation of casein as an example, making predictions on the limitations and future directions (6). The Maillard reaction is a non-enzymatic glycosylation process involving the condensation of carbonyl and ammonium groups between free amino groups of proteins and carbonyl groups of reducing sugars (7). This process significantly enhances the antioxidant capabilities of oxidized peptides and offers advantages such as simplicity (8), low toxicity, and high efficiency, rendering it a preferred glycosylation method (9).

Functional monosaccharides are monosaccharides exhibiting particular biological functions (e.g., antioxidant, anti-inflammatory). This work involved the glycosylation of RPH with arabinose, xylose, and fructose. Previous studies have indicated that these monosaccharides may enhance protein products' antioxidant and functional attributes. Arabinose glycosylation effectively decreased fat oxidation (10). Wang et al. found that the antioxidant capacity of whey protein and xylose glycosylation products was significantly increased (11). Fructose glycosylation diminished the sensitivity of wheat gluten proteins (12). This study utilized the glycosylation of rice protein hydrolysate with certain functional monosaccharides to elucidate their connection with antioxidant capabilities. While the antioxidant improvement of RPH by modifications like xylose has been documented, the structural interactions among various monosaccharides (e.g., xylose, fructose, and arabinose) and their synergistic mechanisms both *in vitro* and *in vivo* remain unclear.

This work involved the production of three different glycosylation products of RPH using the Maillard reaction and assessed the effect of glycosylation modification on external antioxidant ability. A zebrafish model was created to evaluate the *in vivo* antioxidant properties, with reactive oxygen species distribution identified via fluorescent staining. This study establishes a theoretical and technical framework for the processing and production of functional glycosylated RPH, thereby enhancing the industrial applicability and economic worth of rice protein. Moreover, as a sustainable and eco-friendly initiative, it diminishes trial-and-error expenses and curtails resource wastage, enhancing ecologically responsible research methodologies.

2 Materials and methods

2.1 Experimental materials

Rice protein powder, with a crude protein content of 80%, was obtained from Xinyang Mufan Biotechnology Co. Trypsin, derived from bovine pancreas (1:250), was supplied by Beijing Bailing Wei Technology Co. Fructose, xylose, and arabinose (98%) were purchased from Shanghai McLean Biochemical Technology Co. Ferrozine (97%) and 1,10-phenanthroline (o-diazaphene, 99%) were acquired from Shanghai Macklin Biochemical Technology Co. and Sinopharm Chemical Reagent Co., respectively. DPPH• (97%) was sourced from Teichai (Shanghai) Chemical Industry Development Co., and $ABTS^{\bullet+}$ (98%) came from Shanghai Aladdin Biochemical Technology Co. Glutathione (GSH, 99%) and ROS Measurement Kits (chemiluminescence method), along with T-SOD kits, were provided by Beijing Bailing Wei Technology Co. and Nanjing Jianjian Bioengineering Institute, respectively. The bicinchoninic acid (BCA) kit, CAT kit, and MDA kit were supplied by Beijing Solepol Technology Co. Other chemical reagents, of analytical purity, were obtained from Sinopharm Chemical Reagent Co.

2.2 Instruments and equipment

An electronic balance (model AX224ZH) was used from OHAUS Instruments (Changzhou) Co. A medical centrifuge (model TG16-WS) was provided by Changsha Hi-Tech Industrial Development Zone Xiangyi Centrifuge Instrument Co. The magnetic stirring water bath (model HCJ-2E) and the magnetic stirrer (model 8S-1) were supplied by Changzhou Enpei Instrument Manufacturing Co. and Changzhou Guozhi Instrument Manufacturing Co., respectively. The freeze-dryer (model LGJ-25C) was from Sihuan Frui Keji Science and Technology Development Co. The pH meter was provided by METTLER TOLEDO INSTRUMENTS (SHANGHAI) CO. An optical absorption full wavelength enzyme labeling instrument (ReadMax 1900) was used from Shanghai Sempervision Biotechnology Co. The particle size analyzer Dynamic Light Scattering (DLS) was a product of Brookhaven Instruments, United States. The Ultraviolet (UV) spectrophotometer (model UV1800) was from Shimadzu International Trading (Shanghai) Co. A Fourier Transform Infrared Spectrometer (model NicoletiS10) was utilized, provided by Shanghai Zequan Instrument Co.

2.3 Preparation of RPH

Modified from previously documented procedures (13, 14), 67 g of rice protein powder were dissolved in 1000 mL of deionized water to form a 1 g/15 mL solution. The solution was stirred at room temperature for 2 h, the pH was adjusted to 8, and then heated in a water bath at 50°C for 15 min. Trypsin was added at an enzyme-to-substrate ratio of 1:100, and the enzymatic reaction was maintained at 50°C for 60 min with a stable pH of 8. After the reaction, the mixture was heated to 95°C for 15 min to deactivate the enzyme, cooled rapidly in an ice bath, and the pH was adjusted to neutral. Following centrifugation (3,500 rpm, 10 min), the supernatant was lyophilized and reserved. The degree of hydrolysis (DH) was determined by the pH-stat method (15), calculating DH according to Equation (1).

$$DH = \frac{h}{h_{tot}} \times 100\% = B \times N_b \frac{1}{\alpha} \times \frac{1}{M_p} \frac{1}{h_{tot}} \times 100\% \quad (1)$$

In the formula:

B, volume of NaOH consumed (mL); N_b, concentration of NaOH (mol/L); α, dissociation degree of α-NH_3^+ at pH = 8 and 50°C under enzymatic hydrolysis conditions is 0.885; M_p, total protein content in the substrate (g); h_{tot}, Theoretical millimoles of peptide bonds per gram of rice protein (7.40 meq/g).

2.4 Preparation of glycosylated rice protein hydrolysates

Following the method described in the literature (16) with slight modifications, 2.0 g of sugar and 1.0 g of rice protein digest were weighed, dissolved in 200 mL deionized water, stirred thoroughly, and the pH was set to 7.0. The mixture was reacted in a magnetic stirrer water bath at 80°C for 4 h to produce RPH-F, RPH-X, and RPH-A. Subsequently, it was cooled in an ice bath to room temperature and the samples were dialyzed at low temperature for 24 h. The dialysate was freeze-dried for use.

2.5 Structural characterization of glycosylation products

2.5.1 Particle size determination

Following the method described in the literature (16, 17) with slight modifications. To examine the impact of glycosylation modification on the conformation of RPH, the average hydrodynamic particle sizes of the samples were assessed using DLS, which operates on the principle of Brownian motion, calculating diffusion coefficients and inferring size distributions by measuring the fluctuation rate of light scattered by the particles in solution. Take 400 μL of dialysate from enzymatic and glycosylated samples respectively, dilute 10 times, and detect particle size using an analyzer. Equilibrate samples for 10 min and scan each three times for the average particle size.

2.5.2 Determination of grafting degree

Following the method described in the literature (16, 18) with slight modifications. The decrease in free amino acid (FAA) levels, indicative of the glycosylation process, was quantified using O-Phthalaldehyde (OPA). For the analysis, 200 μL aliquots of solutions (RPH-F, RPH-X, RPH-A) were transferred to test tubes. Each sample was combined with 4 mL of OPA reagent and incubated at 35°C for 2 min within a water bath. Subsequently, absorbance at 340 nm was recorded. A control sample of 200 μL RPH was subjected to the same experimental conditions. The degree of grafting (DG) indicates the decrease of free amino groups in glycosylation reactions, with higher DG values indicating enhanced covalent binding effectiveness of sugar molecules to proteins. This work employed the OPA method to ascertain DG, with the objective of identifying the best monosaccharide type (e.g., xylose DG = 16.38%) for further functional examination.

To prepare the OPA reagent, weigh 40 mg of OPA and dissolve it in 1 mL of methanol. Subsequently, add 2.50 mL of a 20% SDS solution, 25 mL of a 0.10 mol/L borax solution, and 100 μL of β-mercaptoethanol in that order. Finally, dilute the mixture to a total volume of 50 mL with distilled water.

The degree of grafting (DG) was calculated using Equation (2).

$$DG = \frac{(A_0 - A_1)}{A_0} \times 100\% \quad (2)$$

In the formula:

A_0, Absorbance value of the blank sample at 340 nm; A_1, Absorbance value of the sample at 340 nm.

2.5.3 Fourier transform infrared absorption spectra

Following a method adjusted from (19, 20), four freeze-dried samples (RPH, RPH-F, RPH-X, RPH-A) were mixed and ground with potassium bromide powder at a specific mass ratio. The mixture was pressed into a uniform, transparent flake and analyzed using a Fourier Transform Infrared (FTIR) Spectrometer, scanning from 4,000 cm^{-1}-400 cm^{-1} at a resolution of 2 cm^{-1}.

2.5.4 Ultraviolet spectroscopy

Using the method described in reference (16) with minor modifications, RPH, RPH-F, RPH-X, and RPH-A were each dispersed in a phosphate buffer solution (pH 7.0, 50 mmol/L) at a concentration of 0.50 mg/mL. Absorbance scans were performed using a UV–visible spectrophotometer across the wavelength range of 200–600 nm.

2.6 *In vitro* antioxidant activity assay

2.6.1 Fe^{2+} chelating capacity

Adapting the method from literature (21) with slight modifications, 0.5 mL of sample solutions (mass concentrations: 6, 3, 1.5, 0.75, and 0.375 mg/mL) were taken into 5 mL centrifugal tubes. Then, 3.20 mL of distilled water and 0.10 mL of 2 mmol/L $FeCl_2$ solution were added successively, shaken well, and left for 3 min. Next, 2 mL of 5 mmol/L phenanthroline solution was added, and the reaction occurred at 25°C for 10 min. Absorbance was measured at 562 nm with an enzyme counter. Deionized water served as the blank control and glutathione as the positive control in three parallel experiments. The Fe^{2+} chelating capacity of the samples was calculated according to Equation (3).

$$P = \frac{(A_0 - A_s)}{A_0} \times 100\% \quad (3)$$

In the formula:

P, Fe^{2+} chelating capacity; A_0, Absorbance of the blank group measured at 562 nm; A_S, Absorbance of the experimental group measured at 562 nm.

2.6.2 Hydroxyl radical scavenging capacity

Referring to the method in the literature (22) with slight modifications, the reagents were added according to the combinations

in the (Table 1), where the concentrations of the sample solution to be tested were 6, 3, 1.5, 0.75, and 0.375 mg/mL in that order.

The solutions were thoroughly mixed, and reactions were conducted for 60 min at 37°C in a water bath. Absorbance at 536 nm was measured, with the procedure repeated in triplicate. The scavenging activity of the samples against hydroxyl radicals was quantified according to Equation (4).

$$P = \frac{A_2 - A_1}{A_0 - A_1} \times 100\% \quad (4)$$

In the formula:

P, hydroxyl radical scavenging rate; A_0, absorbance measured in the blank group; A_1, Absorbance measured for the control; A_2, absorbance measured by the experimental group.

2.6.3 Superoxide anion radical scavenging capacity

Following modifications from literature (22), 1.0 mL of sample solutions was placed into a 10 mL centrifuge tube. Each tube received 3.00 mL of 50 mmol/L Tris–HCl buffer (pH 8.2), reacted at 25°C for 20 min, followed by the addition of 3.00 mL of 7 mmol/L pyrogallol solution, and reacted for another 5 min. The reaction was terminated with 1 mL of concentrated HCl, and absorbance was measured at 325 nm. This procedure was repeated in triplicate, and the superoxide anion radical scavenging rate was determined according to Equation (5).

$$P = \frac{A_0 - (A_1 - A_2)}{A_0} \times 100\% \quad (5)$$

In the formula:

P, superoxide anion radical scavenging rate; A_0, absorbance at 325 nm of deionized water instead of sample solution; A_1, absorbance of the sample solution at 325 nm; A_2, absorbance at 325 nm of the sample solution without pyrogallol added.

TABLE 1 Addition of hydroxyl radical regent (mL).

Solution name	Experimental group	Control	Blank group
o-Diazophene solution (1.5 mmol/L)	1.0	1.0	1.0
Phosphate buffer solution (pH 7.4)	2.0	2.0	2.0
Distilled water	–	1.0	1.0
Ferrous sulfate solution (1.5 mmol/L)	1.0	1.0	1.0
0.02% hydrogen peroxide solution	1.0	1.0	–
Distilled water	–	–	1.0
Sample solution to be measured	1.0	–	–

2.6.4 DPPH• scavenging rate

Following the method described in the literature (16, 23) with slight modifications. In the experimental system, 3.0 mL of DPPH• solution was added with 1.0 mL of the sample solution for the experimental group, while anhydrous ethanol substituted the DPPH• solution in the control group, and the sample solvent replaced the sample in the blank group. The concentrations of the sample solution under investigation were 6, 3, 1.5, 0.75, and 0.375 mg/mL, respectively. Sample solutions were formulated with differing concentrations. The components were properly mixed and permitted to react for 60 min in darkness prior to measuring the absorbance at 517 nm. Deionized water functioned as the zero calibration standard, while glutathione served as the positive control. The method was repeated thrice, and the scavenging efficacy against DPPH• was determined using Equation (6).

$$P = \left(1 - \frac{A_s - A_c}{A_b}\right) \times 100\% \quad (6)$$

In the formula:

P, DPPH• scavenging rate; A_s, absorbance measured by the experimental group; A_c, absorbance measured for the control; A_b, absorbance measured in the blank group.

2.6.5 ABTS•$^+$ scavenging rate

Following the method described in the literature (16, 24) with slight modifications. In the experimental group, 3.6 mL of ABTS•$^+$ solution was combined with 0.4 mL of sample solution. The control group substituted the samples with solvent, with the concentrations of the test solution being 6, 3, 1.5, 0.75, and 0.375 mg/mL, respectively, mixed thoroughly, and allowed to react for 5 min in darkness. Absorbance was subsequently quantified at 734 nm, utilizing deionized water for zero calibration and glutathione as the positive control. The method was conducted in triplicate, and the scavenging activity against ABTS•$^+$ was determined using Equation (7).

$$P = \left(\frac{A_b - A_s}{A_b}\right) \times 100\% \quad (7)$$

In the formula:

P, ABTS•$^+$ scavenging rate; A_b, absorbance measured in the blank group; A_s, absorbance measured by the experimental group.

2.7 *In vivo* antioxidant activity assay

2.7.1 Zebrafish culture and collection of zygotic embryos

Wild-type AB strain zebrafish were employed in this study. Feeding of zebrafish was conducted separately by sex in the breeding tank, with one spoonful of shelled Toyon shrimp eggs provided bi-daily at 09:00 and 17:00. The temperature was regulated at 28°C ± 0.5°C, and a light–dark cycle of 14 h of light and 10 h of darkness was maintained. Zebrafish embryos were obtained by the natural mating spawning technique. At 18:30 on the eve of breeding, male and female zebrafish were positioned in a 1:1 ratio on either side

of the breeding tank, divided by a baffle, and maintained in darkness overnight. At 08:30 the following day, the barriers were dismantled and the lighting system was activated to facilitate zebrafish mating and spawning. Zebrafish embryos were gathered and maintained in an incubator at 28.5°C.

2.7.2 Assessment of the provided dosage

Juvenile fish (3 day post fertilization, dpf) were placed randomly in 6-well plates (4 mL solution volume/well, 30 fish/well). The test group was treated with RPH-A solutions at concentrations of 50.0, 100.0, 200.0, 400.0, and 800.0 μg/mL. Model and normal control groups were established. Except for the normal group, all others were exposed to 300 μM hydrogen peroxide (H_2O_2) to induce oxidative damage in zebrafish. After 24 h, the number of deceased fish in each group was recorded. The highest RPH-A concentration without causing fish death or morphological abnormalities was determined as the maximum toxic concentration (MTC).

2.7.3 *In vivo* ROS detection and antioxidant evaluation in zebrafish

Slightly modified with reference to (25). Juvenile zebrafish (3 dpf) were divided randomly into four groups: Control (blank control group), Model (300 μM H_2O_2), RPH group (200 μg/mL RPH + 300 μM H_2O_2), and RPH-A group (200 μg/mL RPH-A + 300 μM H_2O_2), with three replicates in each group. Samples were incubated with a 40 μg/mL fluorescent probe for 20 min for ROS labeling, followed by photography using an *in vivo* fluorescence microscope to assess fluorescence intensity.

2.7.4 Determination of peroxidase activity in zebrafish

Juvenile zebrafish (3 dpf, normal development) were divided randomly into four groups: Control (blank control group), Model (300 μM H_2O_2), GSH group (20 μg/mL glutathione + 300 μM H_2O_2), and RPH-A group (200 μg/mL RPH-A + 300 μM H_2O_2), with three replicates for each. The treatments were conducted over 4 days using the protocols provided with the MDA, CAT, and T-SOD kits. The MDA concentration, CAT activity, and T-SOD activity were measured separately using a UV spectrophotometer.

2.8 Statistical analysis

Data were analyzed using SPSS software, with results presented as "mean ± standard deviation (SD)." A one-way analysis of variance (ANOVA) was utilized to assess differences among groups, considering $p < 0.05$ as statistically significant.

3 Results and discussion

3.1 Degree of hydrolysis of enzymes

The hydrolysis degree of rice protein via trypsin in this experiment was 5.98%. According to the optimization experiments of Yang et al. (26), the hydrolysis degree of rice protein by trypsin hydrolysis can reach 54.0% under optimum conditions. A strong correlation exists between the extent of hydrolysis of enzymatic hydrolysate and factors such as substrate concentration, starting pH, enzyme quantity, reaction temperature, and hydrolysis time. Moreover, Ma et al. (27) discovered that excessive hydrolysis compromises the structure of enhanced rice protein, resulting in diminished heat resistance. Additionally, varying degrees of hydrolysis through different restriction enzymes also influenced the *in vitro* antioxidant activity of RPH (28).

3.2 Particle size determination

Glycosylation increased the average particle size of all products: specifically, RPH-F was enlarged by over 3.5 times relative to RPH, RPH-X by over 1.6 times, and RPH-A by up to 1.2 times compared to RPH (Figure 1). These changes suggest that modified RPHs adopt a looser structural organization. Ma et al. noted that the addition of monosaccharide molecules alters the conformation of protein, leading to an increase in particle size (29). Variations in particle size among glycosylated products might stem from the differing accessibility of functional sugars to various protein sites (30). The larger the molecular weight of the sugar, the greater the obstruction to protein compactness. Given fructose's larger molecular weight, RPH-F exhibited the greatest increase in particle size under identical glycosylation condition. Xylose and arabinose exhibit variations in their glycosylation sites on proteins; arabinose preferentially binds to the hydroxyl or amine groups of proteins, while xylose may be associated through distinct glycosidic linkages. This may lead to RPH-X forming more expansive, less compact structures during glycosylation, whereas RPH-A produces denser formations (31).

3.3 Grafting degree determination

The grafting degree for RPH-X, derived from the reaction between rice protein digest and xylose, reached a maximum of 16.38% under identical experimental conditions (Figure 2), consistent with previous studies (16). The physicochemical and functional characteristics of

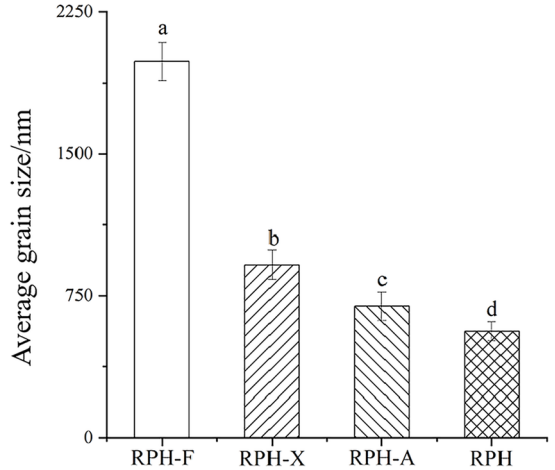

FIGURE 1
Effects of different glycosylation reactions on the average particle size of RPH.

grafted rice protein glycosylation products were comparable. A high grafting degree suggests a reduction in FAA content in the glycosylated product, indicating that certain amino acids are covalently bonded to sugars (32). The binding capacity of RPH to the three sugars was ranked as follows: xylose > fructose > arabinose. This hierarchy may be attributed to the chemical structures of the sugars and their affinity for proteins. The relatively lower grafting efficiency of fructose and arabinose could be due to structural differences that reduce their binding capacity (33). The aldehyde group of xylose demonstrates higher reactivity compared to the ketone group of arabinose, whereas the cyclic structure of arabinose reduces its accessibility to the peptide chain, resulting in a difference in grafting degree (RPH-X: 16.38% vs. RPH-A: 8.72%) (34). Xylose had the greatest glycosylation efficiency, presumably due to the elevated reactivity of its aldehyde group, which promotes enhanced interactions with proteins.

3.4 Fourier infrared absorption spectra

FTIR spectroscopy is employed for protein structural analysis, as it detects characteristic absorption peaks in the mid-infrared region, reflecting changes in the peptide chain structure. The wavelength range of 3,500–3,000 cm^{-1} corresponds to the characteristic absorption peak of -OH groups (Figure 3). Compared to RPH, the three glycosylation products exhibited enhanced absorption intensity (decreased transmittance) and a slight blue shift in the absorption peaks at 3500–3000 cm^{-1}. This shift indicates the stretching vibration of the -OH group and the formation of new -OH bonds, suggesting the occurrence of a glycosylation reaction. Since sugar molecules are rich in -OH groups, their attachment to RPH via covalent bonds leads to an increased presence of -OH groups.

Moreover, the highly polar nature of -OH groups enable them to establish hydrogen bonds, which accounts for the wider absorption peaks ranging from 3,650–3,200 cm^{-1} in the conjugates (35). Absorption peaks found between 1,000–1,070 cm^{-1} typically reflect the C-O-C stretching vibrations and the presence of glycan rings within sugar molecules (36). At 1050 cm^{-1}, a notable increase in absorption peak intensity was evident across all three glycosylated products, suggesting that the sugar molecules prompted vibrations in the protein side chains as a result of the glycosylation process. In addition, each of the three glycosylation products exhibited a distinct absorption peak between 1,380–1,410 cm^{-1}. This peak, attributable to the -CN stretching vibration, arises from carbonyl-ammonia condensation (37) and indicates an augmentation in glycosidic bond formation.

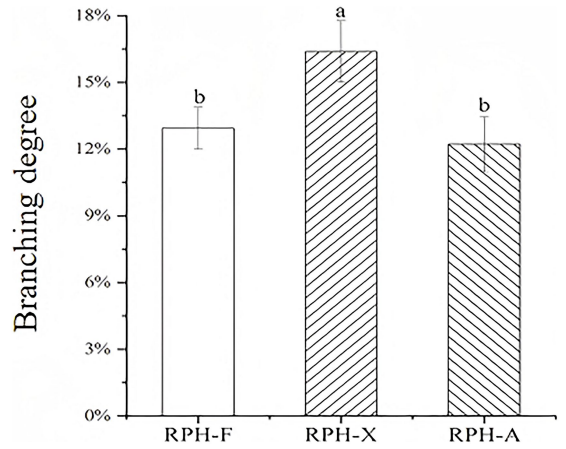

FIGURE 2
Grafting degrees of different glycosylation reaction products.

3.5 Ultraviolet spectroscopy

Aromatic amino acids, such as tyrosine, tryptophan, and phenylalanine, present in RPH (38), absorb ultraviolet light at specific wavelengths, particularly at 225 nm and 280 nm (Figure 4). The glycosylation product showed a slight blue shift in UV absorption, peaking at 221 nm. This shift suggests that glycosylation may alter the protein's three-dimensional structure, especially the conformation of peptide chains. Likely due to the Maillard reaction, which forms covalent bonds between amino acids and sugars, these alterations modify molecular interactions. Consequently, structural changes expose certain hydrophobic amino acid side chains, increasing their interaction with the environment. This exposure might explain the enhanced peak in UV absorption (9).

3.6 *In vitro* antioxidant activity assay

3.6.1 Fe^{2+} chelating capacity

The Fe^{2+} chelating ability of both enzymatic hydrolysates and glycosylation products increased with rising concentrations, from 0.375 to 6 mg/mL. A significant rise of 6.23% in Fe^{2+} chelating capacity was noted at a 0.75 mg/mL concentration of RPH-F (Figure 5), indicating superior antioxidant activity in RPH-F compared to other glycosylated variants. This enhancement is likely due to the unique structure of RPH-F formed during glycosylation and the molecular structure of xylose, which enhances its Fe^{2+} binding. The exposure of carbonyl groups on amino acid residues, which possess strong coordination capabilities, allows for more effective Fe^{2+} complex formation (39). By chelating Fe^{2+}, glycosylated RPH may reduce oxidative damage by preventing the generation of free radicals (20). Furthermore, glycosylation alters the protein's spatial conformation, exposing more hydrophilic and hydrophobic regions, which improves its chelating capability and antioxidant properties.

3.6.2 Hydroxyl radical scavenging capacity

Hydroxyl radicals, capable of causing extensive damage to human cells and leading to lipid peroxidation (23), are more effectively scavenged by glycosylated products. The scavenging activity of these products increased with concentration. Among them, RPH-F showed the least effective •OH scavenging capability (Figure 6A). This effect is attributable to the glycosylation products acting as chelating agents that bind with metal ions such as Fe^{2+}, inhibiting hydroxyl radical production and consequently reducing oxidation. The variation in antioxidant properties among glycosylated products is linked to the type of glycosyl groups and the degree of modification (40). Zhang et al. investigated Maillard reaction products of derived from soy protein isolate with L-arabinose and D-galactose, demonstrating that glycosylation with L-arabinose resulted in superior antioxidant

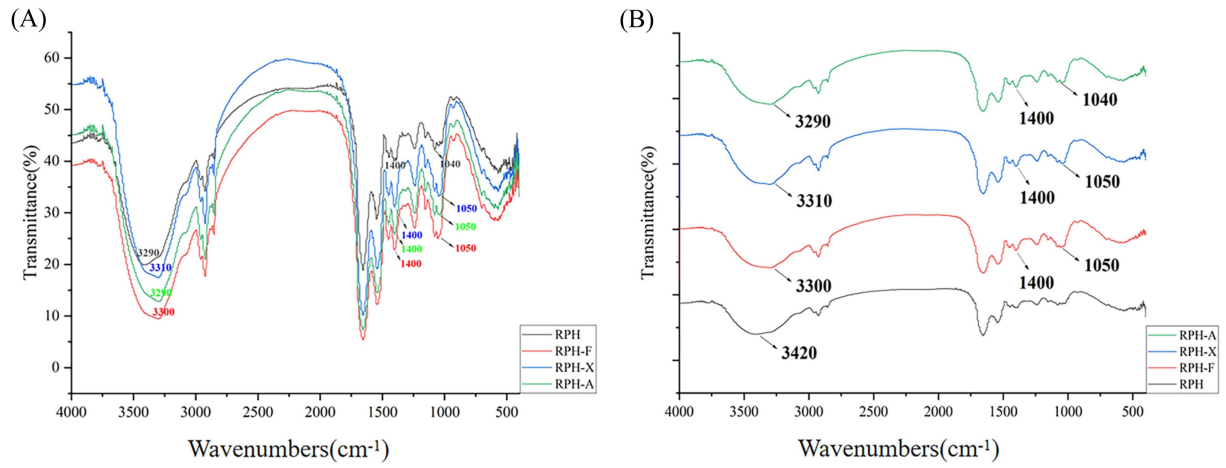

FIGURE 3
(A) Infrared spectra of RPH and its glycosylated products. **(B)** Infrared spectral expansion of RPH and its glycosylated products.

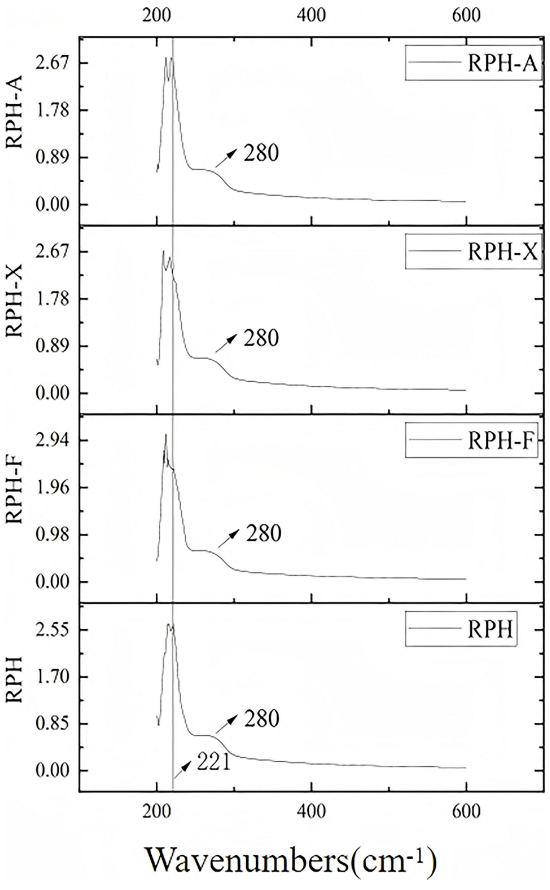

FIGURE 4
UV spectra of RPH and its glycosylated products.

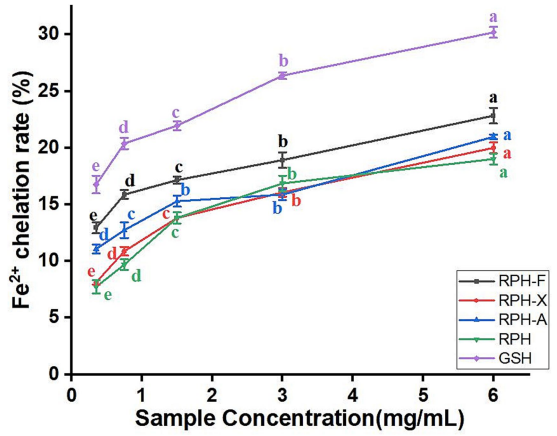

FIGURE 5
Fe^{2+}chelating ability of different glycosylation products.

activity, primarily due to its higherdegree of glycation and more substantial effects on protein conformation (41). Similarly, Xiao et al. reported that solid-state fermentation significantly enhanced the free radical scavenging capacity of buckwheat by releasing bound phenolic compounds through microbial hydrolytic enzymes (42). Although native rice protein typically exhibits limited antioxidant activity, its simple structure, minimal branching, and high content of reactive amino acids such as lysine and arginine, render it particularly suitable for non-enzymatic glycosylation, enabling the formation of uniform and stable glycosylation products (33).

3.6.3 Superoxide anion radical scavenging capacity

Superoxide anion radicals, which can evolve into highly reactive hydroxyl radicals (43), were tested for scavenging potential. Even at a maximum concentration of 6 mg/mL, the scavenging capacity of RPH did not exceed 15% (Figure 6B). However, glycosylated samples displayed a significant improvement, with RPH-F showing the most notable enhancement. This indicates that glycosylation effectively enhances the antioxidant properties of RPH. This is consistent with the findings of Wang et al., who demonstrated that

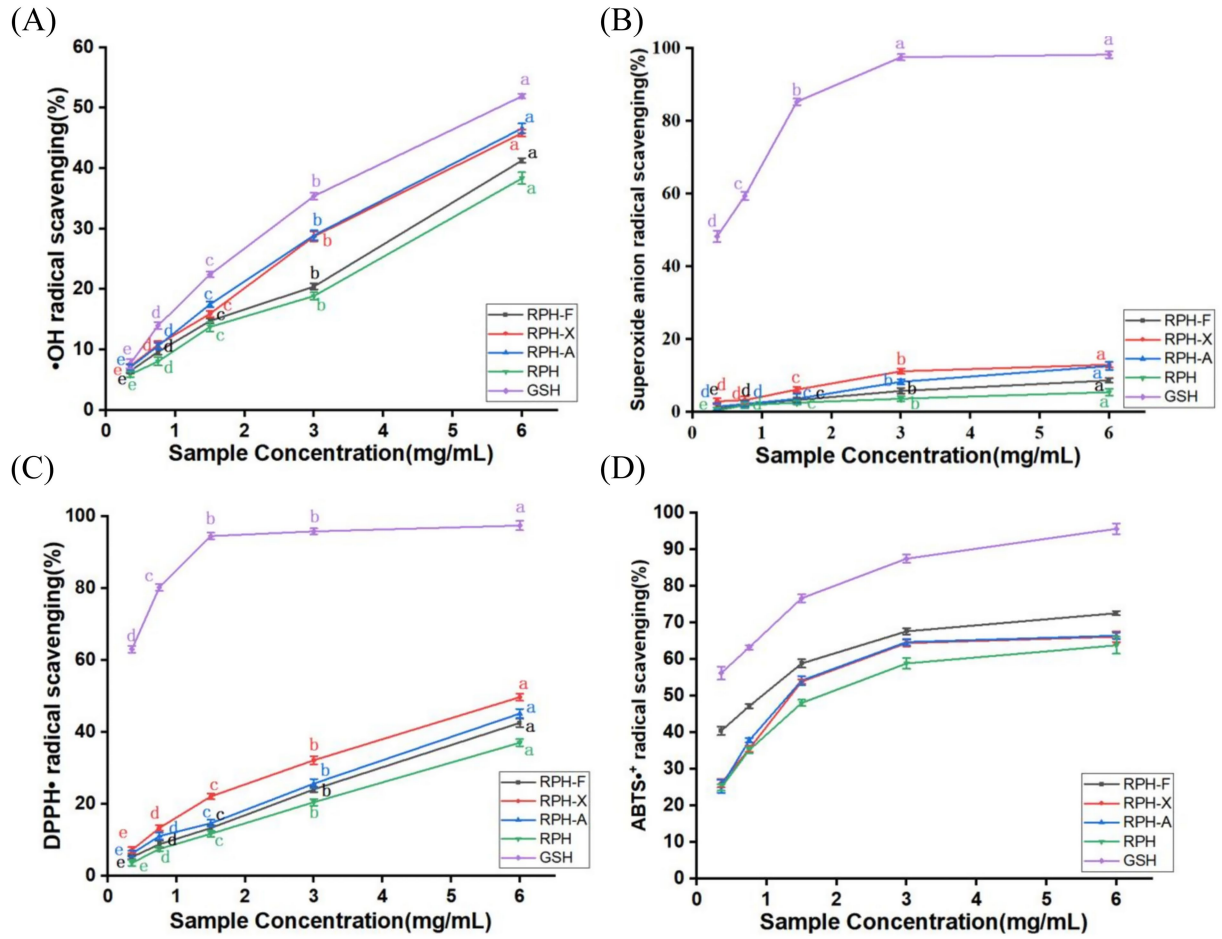

FIGURE 6
(A) •OH radical scavenging rate of different glycosylation products. **(B)** Superoxide anion radical scavenging rate of different glycosylation products. **(C)** Scavenging rate of DPPH• by different glycosylation products. **(D)** Scavenging rate of ABTS•⁺ by different glycosylation products.

glycosylation of yak casein with glucose via the Maillard reaction significantly enhanced its superoxide anion scavenging capacity, and this effect increased proportionally with higher sugar concentrations (44). Additionally, Limsuwanmanee et al. reported a similar observation in a Maillard reaction system involving aquatic by-products and various monosaccharides, finding that glycosylation substantially improved the products' $O_2•^-$ scavenging activity with smaller monosaccharides (such as fructose and glucose) exhibiting more pronounced effects (45). As superoxide anion radicals are precursors to highly reactive substances, their scavenging capacity closely mirrored the trend observed for hydroxyl radicals (Figures 6A,B). Compared to RPH, glycosylation enhanced the superoxide anion radical scavenging ability, likely due to the polyhydroxyl structure of the sugars and the antioxidant-active amino acid residues. These modifications allow the glycosylated products to act as effective hydrogen donors, neutralizing superoxide anion radicals (28). Furthermore, glycosylation modifications have been shown to improve the solubility and stability of proteins, the introduction of hydrophilic hydroxyl groups from sugars increases surface hydrophilicity, thereby enhancing water solubility, enhancing their ability to interact with reactive substances (40).

3.6.4 DPPH• scavenging capacity

DPPH• is a stable nitrogen-centered radical, absorbing maximally at 517 nm. The purple ethanol solution of DPPH•, and its concentration, relate linearly to absorbance. The antioxidant capacity of a substance can thus be determined by measuring its ability to scavenge DPPH• at 517 nm (46). Both RPH and glycosylation products showed increased scavenging activity as the concentration increased, with glycosylation products demonstrating higher DPPH• scavenging rates than the hydrolysates. In this study, we observed a 12.75% increase in the DPPH• scavenging rate of RPH-X (Figure 6C), aligning with the trend of enhanced DPPH• activity reported by Chen et al. in fermented soybeans (47). Wang et al. reported that yak casein glycosylated via the Maillard reaction exhibited significantly greater DPPH• scavenging capacity compared to its native form, with efficacy strongly correlated with the extent of glycation (44). Similarly, Dai et al. demonstrated that enzymatic hydrolysis of wheat gluten with subsequent Maillard glycosylation significantly enhanced its DPPH• scavenging ability, achieving up to 71.71% clearance under optimal conditions (48). Compared with proteins such as casein and gluten, rice protein inherently possesses relatively low antioxidant activity, possibly due to its compact structure and limited hydrophobic group exposure. However, the protein's favorable chemical reactivity allows

substantial improvement of antioxidant properties through glycation. Previous studies have demonstrated that the Maillard reaction markedly enhances DPPH• scavenging capacity by increasing protein hydrophilicity, revealing reactive functional sites, and introducing hydrogen-donating groups (33).

3.6.5 ABTS•$^+$ scavenging capacity

ABTS is oxidized to form ABTS•$^+$, imparting a stable blue-green color with maximum absorption at 734 nm. Antioxidant components react with ABTS•$^+$, leading to discoloration of the reaction system, and the scavenging capacity is calculated (16). The ABTS•$^+$ scavenging capacity of glycosylated rice proteolytic digests progressively increased with increasing concentration within a specific range. Furthermore, the ABTS•$^+$ scavenging capacity of glycosylated rice protein digests exceeded 50%. At a concentration of 3 mg/mL, the scavenging rates of RPH-X, RPH-A, and RPH-F were 60.7, 61.2, and 63.5%, respectively, (Figure 6D). The sequence of ABTS•$^+$ scavenging potency was RPH-F > RPH-A > RPH-X. This enhanced activity of RPH and its derivatives might be due to the formation of more potent free radical-scavenging compounds during glycosylation, potentially similar to black essence-like structures (39). Chen et al. found that solid-state fermentation significantly increased the contents of total phenolics, total flavonoids, and aglycone isoflavones in soybeans, thereby enhancing their scavenging abilities against free radicals such as ABTS•$^+$ and DPPH• (49). These findings further highlight the crucial role of structural modification in improving free radical scavenging capacity. Additionally, the ABTS•$^+$ scavenging rate showed a positive correlation with sample concentration, a pattern consistent with the other antioxidant activity-concentration relationships observed.

3.7 Evaluation of *in vivo* antioxidant effect

3.7.1 Examination of administered dose

As the tolerated concentration of RPH-A in zebrafish is unknown, a preliminary experiment was conducted. For each concentration gradient, 90 zebrafish were selected with three parallel groups established for each concentration. This gradient was used to determine the maximum tolerated concentration (MTC) of the enzyme hydrolysates in zebrafish, providing essential reference data for evaluating their antioxidant efficacy.

As indicated in Table 2 under the experimental conditions, when zebrafish were exposed to RPH-A at concentrations below 200.0 μg/mL, both the experimental and control groups exhibited no deaths or morphological abnormalities. However, as the concentration of RPH-A increased, a gradual increase in zebrafish mortality was observed, suggesting that the toxicity of RPH-A is positively correlated with its concentration. The MTC of RPH-A for zebrafish was established at 200.0 μg/mL, consistent with previous findings (50).

3.7.2 Detection of ROS and evaluation of antioxidant effects in zebrafish

Hydrogen peroxide, a known oxidant, can significantly elevate ROS levels when organisms are exposed to external stressors, exceeding their natural antioxidant defenses and causing oxidative stress. This imbalance may result in considerable cellular damage (51). A common method for detecting ROS in zebrafish involves the use of fluorescent probes, such as dichlorodihydrofluorescein diacetate (DCFH-DA), which crosses cell membranes and is oxidized to fluorescent compounds upon ROS exposure. The antioxidant effect of RPH-A in zebrafish is assessed by measuring fluorescence intensity. The fluorescence intensity results, after continuous exposure for 96 h, are presented below:

Fluorescence intensity is presented in ImageJ as a pixel value, grayscale value, or optical density value. A pixel is the basic unit of an image, and its numerical value represents the intensity.

As depicted in Figure 7 and Table 3 fluorescence intensity in the head, heart, and trunk regions of zebrafish larvae in the model group was significantly higher, confirming successful establishment of the oxidative damage model and elevated ROS levels in the zebrafish. These observations align with findings from Luo et al. (52). The fluorescence intensities in the RPH-A and RPH groups were lower, indicating that both RPH and its glycosylated form, RPH-A, effectively reduced ROS levels in zebrafish. The enhanced bioactivity observed might result from glycation-induced structural modifications that alter cell membrane permeability (53), thereby facilitating deeper tissue penetration. Moreover, glycation-induced conformational stabilization protects critical antioxidant amino acid residues (e.g., Tyr and Trp) from degradation or oxidation, consequently improving their stability and durability (54).

TABLE 2 Experimental result of maximum detectable concentration of zebrafish (n = 30).

Groups	RPH-A sample concentration/(μg/mL)	Zebrafish mortality	Zebrafish mortality rate/%	Phenotype
Normal control group	–	0	0	No apparent abnormality
Model Control group	–	0	0	No apparent abnormality
Test group	50.0	0	0	Similar status to Modeled controls
	100.0	0	0	Similar status to Modeled controls
	200.0	0	0	Similar status to Modeled controls
	400.0	5	17	–
	800.0	30	100	–

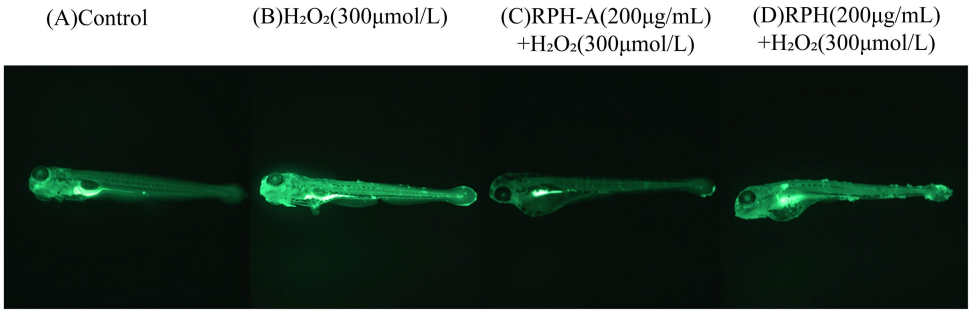

FIGURE 7
Typical diagrams of fluorescence intensity in zebrafish.

TABLE 3 Evaluation experiment results on the antioxidant efficacy of glycosylated enzymatic hydrolysates.

Groups	Fluorescence intensity (pixels, mean±SE)	Relative fluorescence intensity	Antioxidant effect/%
Control	581,453 ± 13684.66	0.015	–
Model	36,507,700 ± 1447285.79	1.000	–
RPH	25,229,703 ± 1476000.38***	0.691	31.39***
RPH-A	6,045,490 ± 432304****	0.170	84.78****

Comparison with model control group, ***$p < 0.001$, ****$p < 0.0001$.

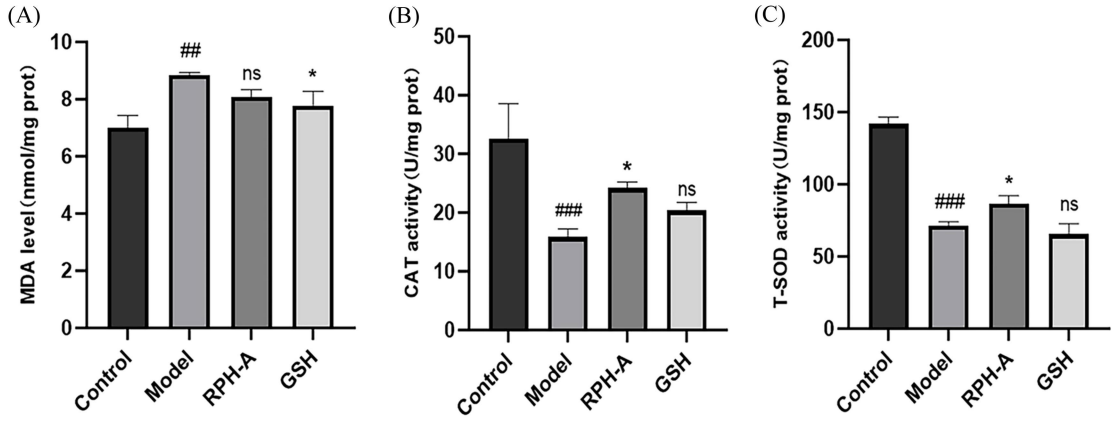

FIGURE 8
Zebrafish body MDA levels and peroxidase activity. **(A)** MDA levels. **(B)** CAT activity. **(C)** T-SOD activity. The * sign indicates a significant difference, *$p < 0.05$ The # sign represents a significant difference in the model control group, # ($p < 0.05$), ## ($p < 0.01$), ### ($p < 0.001$), ns indicates no significant difference ($p > 0.05$).

3.8 Effects of RPH-A on peroxidase activity in zebrafish

MDA levels, indicative of lipid peroxidation and thus oxidative stress, were significantly elevated in the model group (Figure 8A; $p < 0.01$), validating the model's effectiveness (55). Conversely, MDA concentrations were lower in the GSH-treated group, underscoring its protective role against lipid peroxidation.

CAT, prevalent in animals, plants, microbes, and cultured cells, is the predominant H_2O_2 scavenging enzyme and plays a crucial part in the reactive oxygen species scavenging mechanism. In the model group, CAT activity was significantly decreased ($p < 0.001$), suggesting an impairment of the antioxidant defense mechanism. Conversely, in the RPH-A treated group, CAT activity was notably higher ($p < 0.05$; Figure 8B), indicating that RPH-A plays a role in enhancing antioxidant defenses. Additionally, CAT levels in the GSH-treated group exceeded those in the model group, supporting findings from earlier studies (56).

T-SOD is a metalloenzyme prevalent in living organisms. It serves as a crucial oxygen radical scavenger that catalyzes the disproportionation of superoxide anion to produce H_2O_2 and O_2 (50). T-SOD functions as both a superoxide anion scavenging enzyme and a principal H_2O_2-producing enzyme, significantly contributing to the biological antioxidant system. Regarding T-SOD activity, it was substantially reduced in the model group ($p < 0.001$). However,

T-SOD activity was elevated in the RPH-A treated group ($p < 0.05$), demonstrating RPH-A's protective role in zebrafish, as illustrated in Figure 8C. Comparatively, T-SOD levels in the model group and the GSH-treated group showed no significant differences ($p > 0.05$) (57).

4 Conclusion

This study employed a combined enzymatic hydrolysis and glycosylation modification approach to enhance the antioxidant capacity of RPH, which were subsequently evaluated through *in vitro* and *in vivo* assays. Glycosylation significantly enhanced the ability to scavenge free radicals; at a concentration of 6 mg/mL, the DPPH radical scavenging rate of RPH-X was 12.75% greater than that of unglycosylated RPH. Moreover, glycosylated hydrolysates exhibited robust ROS scavenging activity, with an *in vivo* antioxidant efficacy reaching 84.78%. Additionally, glycosylated hydrolysates markedly elevated the activities of antioxidant enzymes, such as CAT and T-SOD. These findings suggest that glycosylated RPH exhibit substantial antioxidant potential in both *in vitro* and *in vivo* contexts, indicating promising applications in the development of functional foods and nutritional supplements. While the study confirmed the antioxidant activity of glycosylation products using the zebrafish model, zebrafish, as a lower vertebrate, possess a physiological environment that markedly differs from that of humans, potentially limiting their ability to accurately replicate the intricate metabolic pathways or prolonged antioxidant effects observed in humans. Future research should aim to validate these findings using mammalian models.

Data availability statement

The datasets presented in this study can be found in online repositories. The names of the repository/repositories and accession number(s) can be found in the article/supplementary material.

Ethics statement

The animal study was approved by Changsha University of Science and Technology. The study was conducted in accordance with the local legislation and institutional requirements.

Author contributions

ZZ: Writing – review & editing, Formal analysis, Data curation, Writing – original draft. XB: Formal analysis, Data curation, Writing – review & editing. LH: Data curation, Writing – review & editing, Formal analysis. YW: Conceptualization, Writing – review & editing, Supervision. WH: Formal analysis, Writing – original draft, Data curation. HWa: Writing – original draft, Conceptualization, Supervision. XZ: Formal analysis, Writing – original draft, Data curation. HWu: Conceptualization, Writing – review & editing, Supervision. DM: Conceptualization, Writing – review & editing, Supervision. LW: Supervision, Conceptualization, Writing – review & editing. QH: Supervision, Writing – review & editing.

Funding

The author(s) declare that financial support was received for the research and/or publication of this article. This research was funded by the National Natural Science Foundation of China (grant number 31972077), the National Innovation and Entrepreneurship Training Program for College Students (grant number S202410536041) and the Science and Technology Innovation Program of Yiyang City in Hunan Province (grant number 2024YY19). This research was funded by the Research Fund in 2024 from Changsha University of Science and Technology.

Acknowledgments

We thank our seniors for their help during the experiment.

Conflict of interest

QH was employed by the company Hunan Zhunong Rice Industry Ltd Co.

The remaining authors declare that the research was conducted in the absence of any commercial or financial relationships that could be construed as a potential conflict of interest.

Generative AI statement

The author(s) declare that no Gen AI was used in the creation of this manuscript.

Publisher's note

References

1. Wang JY, Lu SL, Li RT, Wang Y, Huang LY. Identification and characterization of antioxidant peptides from Chinese dry-cured mutton ham. *J Sci Food Agric*. (2020) 100:1246–55. doi: 10.1002/jsfa.10136

2. Barnham KJ, Masters CL, Bush AI. Neurodegenerative diseases and oxidative stress. *Nat Rev Drug Discov*. (2004) 3:205–14. doi: 10.1038/nrd1330

3. Song LJ, Pan HD, Xu P, Tang RB, Yu LY. Glycosylation modification of glucosamine of soybean protein hydrolysates and its biological activity. *Cereal & Feed Industry*. (2019) 384:28–31. doi: 10.7633/j.issn.1003-6202.2019.04.007

4. Razavian SMH, Kashfi A, Khoshraftar Z. Purification of bovine liver transglutaminase by gel filtration. *Appl Biol Chem*. (2020) 63:6. doi: 10.1186/s13765-020-0490-9

5. Liang LD, Cao WW, Li LL, Ren GY, Chen JL, Xu HS, et al. Research progress in encapsulation of bioactive compounds in protein-polysaccharide non-covalent and covalent complexes. *Food Sci.* (2023) 44:368–76. doi: 10.7506/spkx1002-6630-20221026-274

6. Zeng BH, Hao MZ, Liu GR, Xiong WW, Che HL. Research Progress of casein glycosylation and changes in functional properties. *Sci Technol Food Ind*. (2023) 44:477–84. doi: 10.13386/j.issn1002-0306.2022050351

7. Jia WY, Li TT, Zheng SY, Chen C, Xia YY. Effect of glycosylation modification on the structure of chickpea protein isolate and functional properties. *Sci Technol Food Ind*. (2025) 46:1–11. doi: 10.13386/j.issn1002-0306.2024080197

8. Pirestani S, Nasirpour A, Keramat J, Desobry S. Preparation of chemically modified canola protein isolate with gum Arabic by means of Maillard reaction under wet-heating conditions. *Carbohydr Polym*. (2017) 155:201–7. doi: 10.1016/j.carbpol.2016.08.054

9. Feng HY, Jin H, Gao Y, Zhu XQ, Zhao QS, Liu CH, et al. The effect of (−)-Epigallocatechin-3-Gallate non-covalent interaction with the glycosylated protein on the emulsion property. *Polymers*. (2019) 11:1688. doi: 10.3390/polym11101688

10. Zhang YL, Li X, Cai YL. Study on the effect of Maillard reaction products on antioxidant activity of meat stuffing derived from L-lysine and D-arabinose. *Cai, Cereals Oils*. (2019) 32:26–9. doi: 10.3969/j.issn.1008-9578.2019.09.008

11. Wang WQ, Bao YH, Chen Y. Study on antioxidant property of modification of whey protein. *Food Fermentation Industries*. (2012) 38:62–7. doi: 10.13995/j.cnki.11-1802/ts.2012.03.002

12. Hou TY, Li XL, Hou XN, Tian YN, Rao H, Hao JX. Effect of glycosylation modification on sensitization of wheat gluten protein. *J Chin Cereals Oils Assoc*. (2024) 39:1–8. doi: 10.20048/j.cnki.issn.1003-0174.000775

13. Ren LK, Fan J, Yang Y, Yue Y, Chen FL, Bian X, et al. Enzymatic hydrolysis of broken Rice protein: antioxidant activities by chemical and cellular antioxidant methods. *Front Nutr*. (2021) 8:788078. doi: 10.3389/fnut.2021.788078

14. Yang ZY, Yan JK, Duan YH, Qiao X, Kong ZH, Xu XF. Study on structure and properties of hydrolyzed rice protein with high emulsification properties. *Food Sci Technol*. (2022) 43:129–36. doi: 10.13386/j.issn1002-0306.2022020046

15. Xu YC, Liu CH. Introduction of method for determination of degree of hydrolysis of protein hydrolysates. *Food Res Dev*. (2007) 28:173–6. doi: 10.3969/j.issn.1005-6521.2007.07.053

16. Li LC. Study on the preparation, physicochemical and functional properties of rice protein glycosylated graft products. [master's thesis]. Guangxi: Guangxi University. (2020).

17. Bu D, Tu ZC, Liu GX, Hu YM, Wang H. Effect of glycation with different reducing saccharides effect of glycation with different reducing saccharides. *J Food Sci*. (2022) 43:1–6. doi: 10.7506/spkx1002-6630-20211014-143

18. Wang MY, Bu GH, Xie YJ, Wang Y. Effects of enzymatic hydrolysis combined with glycosylation on the structure and functional characteristics of Peanut protein. *Food R&D, FRD*. (2024) 45:8–15. doi: 10.12161/j.issn.1005-6521.2024.14.002

19. Liu X, Zheng XQ, Liu XL. Effects of Maillard-type glycosylation on antioxidant activity of corn protein hydrolysates. *Food Mach*. (2018) 34:147–51. doi: 10.13652/j.issn.1003-5788.2018.09.030

20. Liu LL, Li Y, Prakash S, Dai XN, Meng YY. Enzymolysis and glycosylation synergistic modified ovalbumin: functional and structural characteristics. *Int J Food Prop*. (2018) 21:395–406. doi: 10.1080/10942912.2018.1424198

21. Peng LL, Chen JW, Cai J, Ding WP, Wu YN. Combined proteases hydrolysis of rice protein and antioxidant activity of the hydrolysates *in vitro*. *J Wuhan Polytech Univ*. (2017) 36:14–22. doi: 10.3969/j.issn.2095-7386.2017.03.003

22. Niu QY. Study on antioxidant properties of glycosylated products of wheat germ protein. *Food Mach*. (2023) 39:32–7. doi: 10.13652/j.spjx.1003.5788.2022.80687

23. Zhai YF, Wang YH, Tang GX, Niu LY, Zhang YY, Xiang QS. Effect of dielectric barrier discharge plasma-assisted glycation on the antioxidant activity of β-lactoglobulin and its structure-activity relationship. *Sci Technol Food Ind*. (2025) 166:1–15. doi: 10.13386/j.issn1002-0306.2024090294

24. JDzoyem JP, Kuete V, McGaw LJ, Jacobus NE. The 15-lipoxygenase inhibitory, antioxidant, antimycobacterial activity and cytotoxicity of fourteen ethnomedicinally used African spices and culinary herbs. *J Ethnopharmacol*. (2014) 156:1–8. doi: 10.1016/j.jep.2014.08.007

25. Zou YX, Fu XT, Duan DL, Xu JC, Gao X, Wang XL. Antioxidant activities of Agaro-oligosaccharides in AAPH-induced zebrafish model. *Sci Technol Food Ind*. (2019) 40:286–98. doi: 10.13386/j.issn1002-0306.2019.04.048.Q

26. Yang Q, Xiong SB, Wang TT, Li FC. Hydrolyzing conditions of rice protein and effects of their hydrolyzing degree on yield of plastein. *J Huazhong Agric Univ*. (2007) 4:565–9. doi: 10.13300/j.cnki.hnlkxb.2007.04.004

27. Ma XY, Chen XX, Hu ZY, Zhu XM, Xiong H, Zhao Q. Effects of restrictive enzymatic hydrolysis on the structural and functional properties and *in vitro* antioxidant activity of rice protein. *J Chin Inst Food Sci Technol*. (2020) 20:53–62. doi: 10.16429/j.1009-7848.2020.11.007

28. Xie HX, Zhang LQ, Chen Q, Hu JW, Zhang P, Xiong H, et al. Combined effects of drying methods and limited enzymatic hydrolysis on the physicochemical and antioxidant properties of rice protein hydrolysates. *Food Biosci*. (2023) 52:102427. doi: 10.1016/j.fbio.2023.102427

29. Ma QP, Wang H, Tu ZC, Wen PW, Hu YM. Effects of ultrasound-assisted glycation on the allergenicity of β-lactoglobulin during digestion. *Food Mach*. (2021) 37:6–11. doi: 10.13652/j.issn.1003-5788.2021.04.002

30. Liu JL. Effect of glycation on the formation and intestinal cell absorption of bovine serum albumin bound quercetin nanoparticle. [dissertation]. Beijing: China Agricultural University. (2017).

31. Herold S, Bishof R, Metz B. Xylanase gene transcription in Trichoderma reesei is triggered by different inducers representing different Hemicellulosic pentose polymers. *EC*. (2013) 12:390–8. doi: 10.1128/EC.00182-12

32. Li RP. The research of grass carp meat protein on the nutrition and structure properties in a microwave field. [master's thesis]. Nanchang: Nanchang University. (2015).

33. Li Y, Zhong F, Ji W, Yokoyama W, Shoemaker CF, Zhu S, et al. Functional properties of Maillard reaction products of rice protein hydrolysates with mono-, oligo- and polysaccharides. *Food Hydrocoll*. (2013) 30:53–60. doi: 10.1016/j.foodhyd.2012.04.013

34. Xu ST, Zhu QJ, Hu Y, Zhou GJ, Zhu JR. Effects of different kinds of sugars on grafting modification for casein glycosylation. *F & FI*. (2019) 45:118–31. doi: 10.13995/j.cnki.11-1802/ts.021709

35. Cheng YH, Mu DC, Feng YY, Xu Z, Wen L, Chen ML, et al. Glycosylation of rice protein with dextran via the Maillard reaction in a macromolecular crowding condition to improve solubility. *J Cereal Sci*. (2022) 103:103374. doi: 10.1016/j.jcs.2021.103374

36. Wang ZC, Cui SW, Yuan DQ, Zheng JQ, An GJ, Zhao XW, et al. Characteristics of saccharide-protein linkage in the enzymatic hydrolysis of rice protein pretreated with high hydrostatic pressure. *Food Sci Technol*. (2013) 34:100–3. doi: 10.13386/j.issn1002-0306.2013.15.053

37. Zhang Y. Study on the *Procambarus clarkii* shell active peptide LPLWPY regulate the antioxidation and lipid metabolism of zebrafish via Keap 1-Nrf2-PPARγ pathway. [master's thesis]. Harbin: Northeast Agricultural University. (2017).

38. Zhang HX, Xia XF, Wang J, Liu YL, Li YY. Functional properties of rice protein and its enzymatic hydrolysates. *Zhongguo Shipin Xuebao*. (2015) 15:63–70. doi: 10.16429/j.1009-7848.2015.08.010

39. Wang XJ, Qu Y, Liu XL, Cong WS. Effects of modification by D-galactosamine on structural properties and antioxidant activities of corn glutelin. *F & M*. (2019) 35:176–80. doi: 10.13652/j.issn.1003-5788.2019.07.034

40. Xu ZW, Zhang YQ, Ocansey DKW, Wang B, Mao F. Glycosylation in cervical Cancer: new insights and clinical implications. *Front Oncol*. (2021) 11:706862. doi: 10.3389/fonc.2021.706862

41. Zhang Q, Dou L, Sun T, Li X, Xue B, Xie J, et al. Physicochemical and functional property of the Maillard reaction products of soy protein isolate with L-arabinose/D-galactose. *J Sci Food Agric*. (2023) 103:7040–9. doi: 10.1002/jsfa.12790

42. Xiao Y, Wu X, Yao X, Chen Y, Ho C-T, He C, et al. Metabolite profiling, antioxidant and α-glucosidase inhibitory activities of buckwheat processed by solid-state fermentation with *Eurotium cristatum* YL-1. *Food Res Int*. (2021) 143:110262. doi: 10.1016/j.foodres.2021.110262

43. Kanatt SR, Chander R, Sharma A. Antioxidant potential of mint (*Mentha spicata* L.) in radiation-processed lamb meat. *Food Chem*. (2007) 100:451–8. doi: 10.1016/j.foodchem.2005.09.066

44. Wang H, Yang J, Yang M, Ji W. Antioxidant activity of Maillard reaction products from a yak casein-glucose model system. *Int Dairy J*. (2019) 91:55–63. doi: 10.1016/j.idairyj.2018.12.010

45. Limsuwanmanee J, Chaijan M, Manurakchinakorn S, Panpipat W, Klomklao S, Benjakul S. Antioxidant activity of Maillard reaction products derived from stingray (*Himantura signifier*) non-protein nitrogenous fraction and sugar model systems. *LWT-Food Sci Technol*. (2014) 57:718–24. doi: 10.1016/j.lwt.2014.01.042

46. Tan Y, Chen P, Xu SH, Zhu J. Determination of DPPH free radical scavenging ability of homemade queen bee larva cream with whitening, anti-aging, and anti-wrinkle functions by the DPPH·assay. *Guangdong Chem Ind*. (2019) 46:143–4. doi: 10.3969/j.issn.1007-1865.2019.18.068

47. Chen Y, Wang Y, Chen J, Tang H, Wang C, Li Z, et al. Bioprocessing of soybeans (*Glycine max* L.) by solid-state fermentation with *Eurotium cristatum* YL-1 improves total phenolic content, isoflavone aglycones, and antioxidant activity. *RSC Adv*. (2020) 10:16928–41. doi: 10.1039/C9RA10344A

48. Dai Y, Li H, Liu X, Wu Q, Ping Y, Chen Z, et al. Effect of enzymolysis combined with Maillard reaction treatment on functional and structural properties of gluten protein. *Int J Biol Macromol*. (2024) 257:128591. doi: 10.1016/j.ijbiomac.2023.128591

49. Chen J, Chen Y, Hu J, He C, Peng X, Li Z, et al. Solid-state fermentation with *Rhizopus oryzae* HC-1 improves the metabolites profiling, antioxidant activity and gut microbiota modulation effect of soybeans. *LWT*. (2023) 187:115253. doi: 10.1016/j.lwt.2023.115253

50. Chen J, Chen YX, Zheng YF, Zhao JW, Yu HL, Zhu JJ, et al. Neuroprotective effects and mechanisms of procyanidins *in vitro* and *in vivo*. *Molecules*. (2021) 26:2963. doi: 10.3390/molecules26102963

51. Pisoschi AM, Pop A. The role of antioxidants in the chemistry of oxidative stress: a review. *Eur J Med Chem*. (2015) 97:55–74. doi: 10.1016/j.ejmech.2015.04.040

52. Luo L, Song L, Zhang XM. Antioxidant effect of Gannan yak milk based on zebrafish model and antioxidant *in vitro*. *Food Ferment Ind*. (2024) 50:133–8. doi: 10.13995/j.cnki.11-1802/ts.038164

53. Kim HM, Kim S, Sim J, Ma BS, Yong I, Jo Y, et al. Glycation-mediated tissue-level remodeling of brain meningeal membrane by aging. *Aging Cell*. (2023) 22:e13805. doi: 10.1111/acel.13805

54. Liu J, Tu ZC, Shao YH, Wang H, Liu GX, Sha XM, et al. Improved antioxidant activity and glycation of α-lactalbumin after ultrasonic pretreatment revealed by high-resolution mass spectrometry. *J Sci Food Agric*. (2017) 65:10317–24. doi: 10.1021/acs.jafc.7b03920

55. Ouyang D, Zhang C, Yang Y, Lin Z, Su LJ. Physicochemical properties and antioxidant activity of polysaccharides from Sargassum fusiforme prepared by six combined enzymatic method. *Food Sci Technol*. (2024) 45:248–57. doi: 10.13386/j.issn1002-0306.2023120014

56. Engineer A, Saiyin T, Greco ER, Feng QP. Say NO to ROS: their roles in embryonic heart development and pathogenesis of congenital heart defects in maternal diabetes. *Antioxidants*. (2019) 8:436. doi: 10.3390/antiox8100436

57. Zhang Y. (2023) Research on comparison of functional properties of soy protein isolate prepared by different saccharification methods. [master's thesis]. Yancheng, Jiangsu, China: Yancheng Institute of Technology. (2023).